Effects of target polycrystalline structure and surface gas coverage on magnetron I–V characteristics

A. Leybovich, T. Kuniya, P. C. Smith, M. B. Hendricks, and D. N. Ruzic

Citation: J. Vac. Sci. Technol. A **12**, 1618 (1994); doi: 10.1116/1.579024
View online: http://dx.doi.org/10.1116/1.579024
View Table of Contents: http://avspublications.org/resource/1/JVTAD6/v12/i4
Published by the AVS: Science & Technology of Materials, Interfaces, and Processing

Related Articles

The Si3N4/TiN Interface: 4. Si3N4/TiN(001) Grown with a −250 V Substrate Bias and Analyzed In situ using Angle-resolved X-ray Photoelectron Spectroscopy
Surf. Sci. Spectra 19, 62 (2012)

The Si3N4/TiN Interface: 1. TiN(001) Grown and Analyzed In situ using Angle-resolved X-ray Photoelectron Spectroscopy
Surf. Sci. Spectra 19, 33 (2012)

The Si3N4/TiN Interface: 5. TiN/Si3N4 Grown and Analyzed In situ using Angle-resolved X-ray Photoelectron Spectroscopy
Surf. Sci. Spectra 19, 72 (2012)

The Si3N4/TiN Interface: 6. Si/TiN(001) Grown and Analyzed In situ using Angle-resolved X-ray Photoelectron Spectroscopy
Surf. Sci. Spectra 19, 82 (2012)

The Si3N4/TiN Interface: 2. Si3N4/TiN(001) Grown with a −7 V Substrate Bias and Analyzed In situ using Angle-resolved X-ray Photoelectron Spectroscopy
Surf. Sci. Spectra 19, 42 (2012)

Additional information on J. Vac. Sci. Technol. A

Journal Homepage: http://avspublications.org/jvsta
Journal Information: http://avspublications.org/jvsta/about/about_the_journal
Top downloads: http://avspublications.org/jvsta/top_20_most_downloaded
Information for Authors: http://avspublications.org/jvsta/authors/information_for_contributors

ADVERTISEMENT

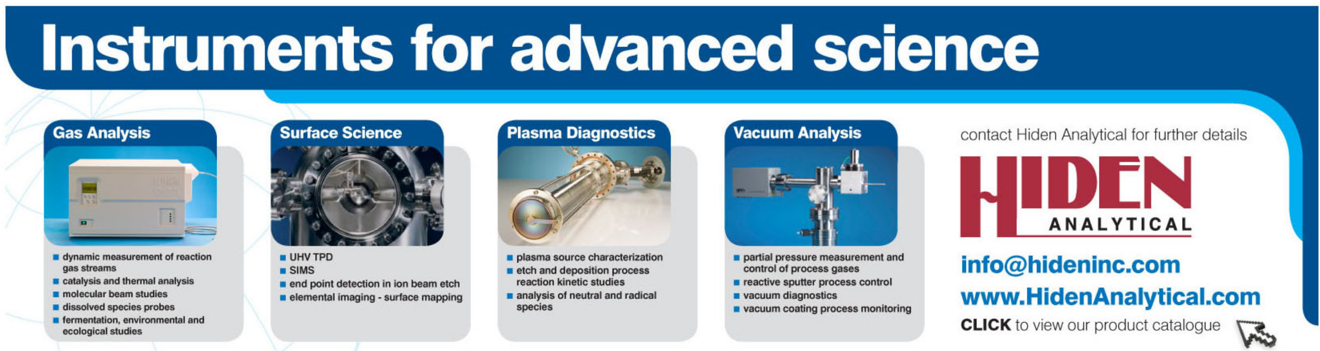

Downloaded 23 Dec 2012 to 192.17.144.173. Redistribution subject to AVS license or copyright; see http://avspublications.org/jvsta/about/rights_and_permissions

Effects of target polycrystalline structure and surface gas coverage on magnetron *I–V* characteristics

A. Leybovich and T. Kuniya
Tosoh SMD, Inc., Grove City, Ohio, 43123

P. C. Smith, M. B. Hendricks, and D. N. Ruzic
University of Illinois, Urbana, Illinois 61801

(Received 6 October 1993; accepted 14 January 1994)

The effects of Al target surface grain structure and surface gas coverage on sputtering magnetron $I-V$ characteristics have been investigated to reveal the net effect of variations in the ion-induced electron emission yield (IIEEY) on $I-V$ characteristics. One (110) single-crystal and three polycrystalline Al–1 wt % Cu targets with the similar (110) crystallographic orientations and grain sizes of 0.25, 0.95, and 5.5 mm were studied. The partial pressures were monitored before, during, and after sputtering. The direct IIEEY was measured under 600–900 eV Ar^+ and He^+ beam bombardment as a function of grain size and gas coverage at specimen temperatures of 19 and 74 °C. The IIEEY measurements demonstrated that both the surface grain structure and the gas coverage affect the electron emission. The direct IIEEY was highest in the small grain size and lowest in the large grain size specimens. An increase in specimen temperature raised the emission yield due to increased chemisorption of residual gas species. In contrast magnetron $I-V$ characteristics suggested the highest IIEEY for medium grain size target. This difference is explained by the combined effect of residual gas adsorption and plasma sheath distortion around surface relief which results in IIEEY increase.

I. INTRODUCTION

The current–voltage ($I-V$) characteristics of sputtering magnetrons play an important role in sputtering plasma characterization. Deposition parameters, process stability, and production reproducibility depend on these $I-V$ characteristics. For example, the deposition rate is generally an increasing function of the discharge current, while the bias voltage affects resputtering by influencing the reflected particle density and distribution.[1,2] The magnetron plasma, like all types of dc glow discharge plasmas, is sustained by a number of elemental ionization and excitation processes. The ionization by electrons ejected from the cathode surface during ion bombardment is a fundamental parameter greatly influencing the self-sustaining nature of the magnetron plasma.[3,4] Namely, the electron emission from the target surface affects the discharge $I-V$ characteristics.

In this article, we report on a series of experiments designed to reveal the effects of target surface gas adsorption on the target emission characteristics. Gas adsorption is studied as a function of target surface grain structure and temperature. The ultimate aim of this study is to determine the nature of $I-V$ curve deviations that are at times observed for targets with similar composition, crystallographic texture, and sputter profile. Sometimes, routine sputtering of identical targets in the same sputtering system exhibits unexpected variations in the $I-V$ characteristics. Therefore, the understanding of the phenomena responsible these I-V curve variations may allow us to improve the consistency of sputtering processes.

The $I-V$ characteristics of dc sputtering magnetrons have been studied by a number of authors.[5–7] Rossnagel[5,6] showed that the target species can affect the bias voltage by a local gas rarefaction in front of the target. He explained the observed phenomenon by the thermalization of sputtered atoms during their interaction with gas particles.

Effects of target crystallographic structure and surface grain relief on sputtering magnetron $I-V$ characteristics was studied by Leybovich *et al.*[7] It was shown that similar targets may exhibit $I-V$ characteristic deviations due to differences in crystallographic structure or in target surface grain relief. The crystallographic structure affects the $I-V$ curves by virtue of the discrepancy in the ion induced electron emission yield (IIEEY) from different crystallographic planes, while the surface grain relief affects the $I-V$ characteristics via secondary electron losses due to their scattering and interception. The present work is a continuation of this study and concerns the effect of aluminum polycrystalline target gas adsorption on $I-V$ characteristics and the IIEEY.

Although the IIEEY from gas-covered metallic surfaces has been studied for various materials (Ta, Pt, W, Ni) and pure adsorbed gases (H_2, N_2, O_2, CO),[8–10] these studies cannot explain the $I-V$ curve deviations observed for aluminum polycrystalline targets. Aluminum (110) single-crystal and polycrystalline targets with similar crystallographic orientations and grain sizes of 0.25, 0.95, and 5.5 mm were examined.

II. EXPERIMENT

The experimental setup used in this study includes two techniques; $I-V$ curve measurements during the magnetron sputtering of actual targets, and ultrahigh vacuum (UHV) IIEEY measurements of specimens made from the target material. The surface exposure conditions in both experiments were comparably maintained.

Downloaded 23 Dec 2012 to 192.17.144.173. Redistribution subject to AVS license or copyright; see http://avspublications.org/jvsta/about/rights_and_permissions

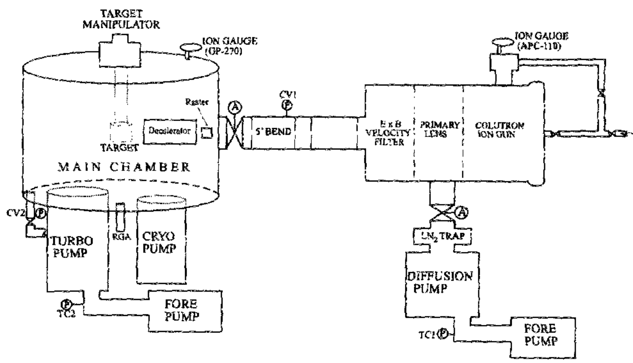

FIG. 1. The experimental apparatus for the IIEEY measurements. System configuration: TC=thermocouple and CV=convectron.

A. Sputtering

Four sputtering targets 5-cm diameter×0.3-cm thickness were used in this experiment: one pure aluminum (99.999%) single-crystal target with (110) crystallographic orientation and three 99.999% purity Al–1 wt % Cu targets with similar (110) preferred crystallographic orientations and grain sizes of 0.25, 0.95, and 5.5 mm. The polycrystalline targets were fabricated and examined as described earlier.[7] Four rectangular specimens 19 mm long×6.3 mm wide made from the target material were also used for direct IIEEY measurements.

The targets were installed into a dc magnetron sputtering system with an unbakeable processing chamber described by Wickersham *et al.*[11] Each target was mechanically clamped to a backing plate of a sputtering source with a magnetic field of 320 G, induced 3 mm above and 15 mm from the source center.[7] Each target was examined at base pressures of 1.0×10^{-4} Pa.

Gas adsorption in this experiment was determined from measured residual gas partial pressures. The residual gas analyzer (RGA) was connected to the sputtering system through a 45-cm-long and 3-cm-diam flexible metallic hose. The base pressure of differentially pumped RGA was maintained at less than 1×10^{-6} Pa. All the analyzed spectra were normalized to the RGA base pressure. The spectra were monitored before, during, and after sputtering. Each target was sputter conditioned at 0.3 A for 15 mins prior to recording the I-V data. Then the system was continuously pumped for 30 mins. High-purity argon at 0.8 Pa was used as the sputtering gas.

B. IIEEY measurements

The IIEEY measurements were carried out with the apparatus described by Smith.[12] Schematically the apparatus is shown in Fig. 1. It consists of two differentially pumped chambers. The ion gun chamber was pumped by a diffusion pump equipped with a liquid-nitrogen cryotrap, while the UHV section was pumped by turbomolecular and cryopumps working together. The UHV section base pressure was around 7×10^{-7} Pa.

A noble gas based Colutron source was used to produce the ions. The ions were extracted, accelerated, and focused into a crossed electrostatic and magnetic field velocity filter. Due to the relatively high pressure in the ion gun (about 1×10^{-3} Pa), the fast neutrals produced by the charge transfer process are filtered by a 5° bend in the system through which the ion beam was electrostatically bent. Before striking the specimen, the ions were decelerated to the desired energy in the range of 600–900 eV and focused into a less than 0.2-mm-diam beam. The ion beam was rastered over the specimen surface in a 1.5×1.5-mm square pattern to obtain uniform exposure. The ion beam energy range was chosen based on three criteria. First, the beam energy range should overlap the ion energies at magnetron sputtering for major industrial applications (conical or planar targets). Second, the energy range should include the expected kinetic emission energy threshold. And third, the ion energy should minimize the effect of space charge on the beam geometrical distortion. The UHV gas medium was monitored using an RGA directly connected to the UHV chamber.

The specimen assembly is presented in Fig. 2. The assembly simultaneously served to hold specimens and to collect incoming ion and emitted electron currents at room or elevated temperatures. The assembly consists of three coaxial electrically insulated cylinders. Thermocouples are mounted in close proximity to the specimens which are fixed on the inner cylinder. The potentials of all the cylinders are chosen to be identical to create a field-free region around the specimen that prevents the ion beam distortion. The two outer

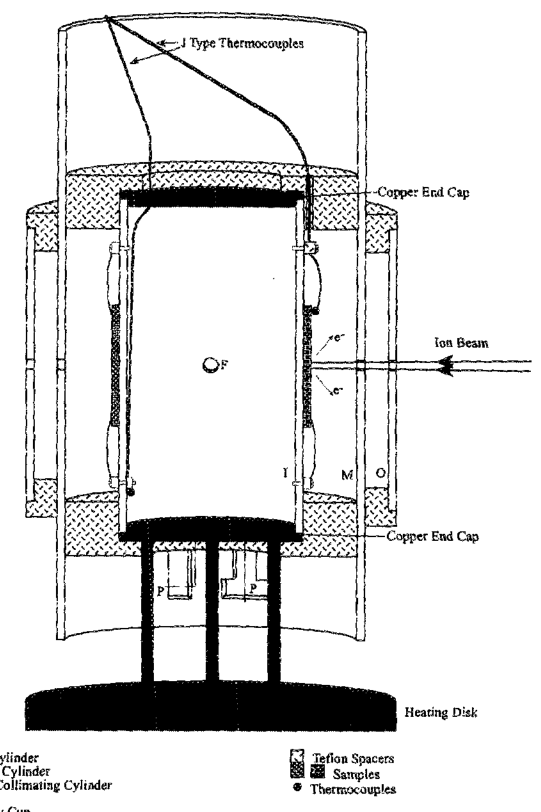

FIG. 2. Specimen assembly.

Downloaded 23 Dec 2012 to 192.17.144.173. Redistribution subject to AVS license or copyright; see http://avspublications.org/jvsta/about/rights_and_permissions

cylinders have coaxial holes for the ion beam to pass through. The incident ion beam passes through a hole in the outer most cylinder where any stray ions are collected, then proceeds through a hole in the middle cylinder without interaction and strikes the specimen. Current collected by the inner cylinder includes two components; the current of incoming primary ions and the current of emitted electrons. The emitted electrons are collected by the middle cylinder. The number of electrons lost back through the entrance hole is taken into account at data analysis. All the currents are measured with the Keithly 416 picoammeter connected to the cylinders. The IIEEY is determined as a ratio between the electron current collected by the middle cylinder and the primary ion current calculated as the difference between the inner and middle cylinder currents.

It may be argued that the IIEEY data determined by this technique are not applicable for magnetron sputtering applications. When the residual gas fluxes on exposed surfaces in magnetron sputtering ($1-10\times10^{16}$ cm^{-2} s^{-1}) are compared with the UHV IIEEY measurements (1×10^{12} cm^{-2} s^{-1}), the observed flux difference of 4–5 orders of magnitude may be considered to be a significant difference in the exposure levels. However, in this experiment, similar exposure conditions were maintained by selecting the same flux ratios for all the species bombarding the surface in sputtering as in IIEEY measurements (residual to process gases and ions to residual gas of 10^{-5} and 10^{-9}, respectively).

III. SPUTTERING EXPERIMENT RESULTS AND DISCUSSION

The $I-V$ characteristics for single-crystal and polycrystalline targets are shown in Fig. 3. As seen, the (110) single-crystal target exhibits the highest bias voltage when compared with polycrystalline targets. The effect of grain size on $I-V$ characteristics is not simple. The voltage is higher for large and slightly lower for medium grain size targets when compared with the small grain size target. Since the crystallographic structure of all the targets is similar, the observed $I-V$ curve variations may be associated with certain dissimilarities in surface gas coverage or in surface grain relief.

The gas adsorption on solids is a function of gas pressure, temperature, and exposure time.[13] The residual gas species is known have a certain thermodynamic privilege for adsorption (chemisorption) in the sputtering medium in spite of their relatively low partial pressures.[14] Therefore, the partial pressure monitoring for gas species before, during, and after sputtering will give us a certain knowledge of adsorption kinetics. The typical RGA data collected in scanning mode are shown in Table I. Since different bypass valves were used to maintain the RGA operational pressure, the RGA data were normalized to the sputtering chamber pressure (Table II). This makes the data comparable for all test conditions.

As seen in Table II, the major peaks before sputtering are water traces (mass numbers 17, 18, and 1) although the N_2/CO peak is also noticeable (mass number 28). During sputtering the partial pressures of water traces are elevated and are still seen against the strong argon peaks with mass numbers 20, 36, 39, 40 (36, 39—argon isotopes). Immediately after sputtering the RGA spectrum is changed dramatically. The molecular hydrogen peak (mass number 2) becomes predominate. After a while the spectrum restores its initial structure although all the peaks are lower in magnitude (Table II).

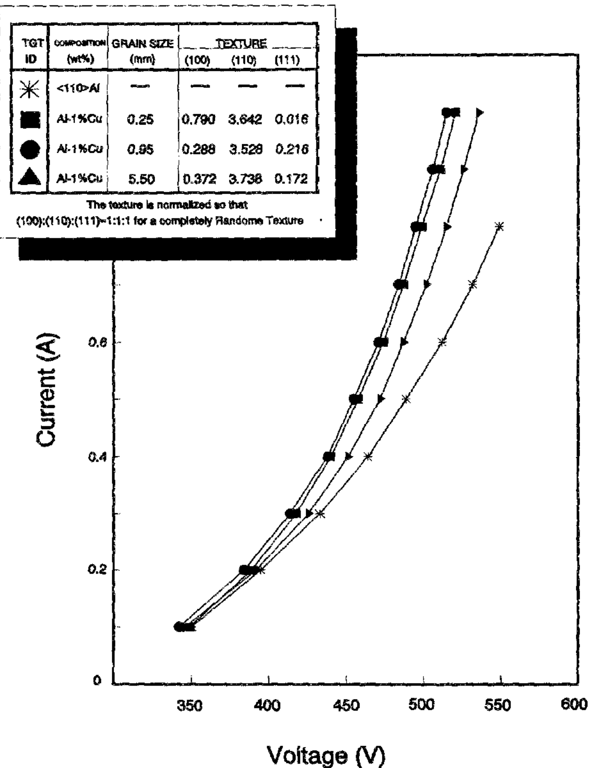

FIG. 3. Effect of grain size on $I-V$ characteristics of Al–1 wt % Cu targets (argon pressure 0.8 Pa).

TABLE I. The typical RGA spectra (eight major peaks) collected in scanning mode: (a) before sputtering, (b) sputtering, (c) 30 min after sputtering, and (d) 90 min after sputtering.

Mass	Torr	Common gases	Mass	Torr	Common gases
	(a)			(b)	
18	0.9×10^{-7}	Water	40	1.5×10^{-6}	Argon
17	2.4×10^{-8}	Water	20	2.4×10^{-7}	Argon
28	1.3×10^{-8}	N_2/CO	18	1.5×10^{-8}	Water
1	1.2×10^{-8}		1	0.8×10^{-8}	
44	4.9×10^{-9}	CO_2	36	5.5×10^{-9}	
2	3.0×10^{-9}	Hydrogen	28	4.0×10^{-9}	N_2/CO
16	2.1×10^{-9}	Oxygen	39	3.7×10^{-9}	
32	2.0×10^{-9}	Oxygen	17	3.6×10^{-9}	Water
	(c)			(d)	
2	0.9×10^{-7}	Hydrogen	18	4.5×10^{-7}	Water
18	4.5×10^{-8}	Water	17	0.9×10^{-7}	Water
1	3.3×10^{-8}		28	1.5×10^{-7}	N_2/CO
28	1.3×10^{-8}	N_2/CO	2	0.7×10^{-8}	Hydrogen
17	3.3×10^{-9}	Water	1	0.6×10^{-8}	
44	3.3×10^{-9}	CO_2	44	1.8×10^{-9}	CO_2
16	1.9×10^{-9}	Oxygen	16	0.9×10^{-9}	Oxygen
29	1.2×10^{-9}		32	0.7×10^{-9}	Oxygen

Downloaded 23 Dec 2012 to 192.17.144.173. Redistribution subject to AVS license or copyright; see http://avspublications.org/jvsta/about/rights_and_permissions

TABLE II. Residual gas partial pressure dynamics at magnetron sputtering.

		Partial pressure (Pa)						
		Before sputtering	During sputtering		After sputtering			
					30 min		90 min	
Species	Mass number	($\times 10^{-5}$)	($\times 10^{-3}$)	Change[a]	($\times 10^{-5}$)	Change	($\times 10^{-5}$)	Change
Water	17, 18	19	3.3	+17	2.7	−0.8	2.7	−0.8
Hydrogen	2, 1	2.4	2.4	+101	7.5	+2.1	0.7	−1.4
N_2/CO	28	2.0	0.9	+46	0.7	−0.6	0.4	+0.8

[a]Change given in multiples of the partial pressure before sputtering.

An explanation for the residual gas partial pressure changes can be found using the published data for the gas adsorption by aluminum.[14] Not all the background species are adsorbed on aluminum identically. The H_2O, CO, O_2 species are able to be adsorbed only on pure aluminum (as well as on pure copper and their alloys), while the H_2, N_2, CO_2 species are not adsorbed. In contrast, the oxidized aluminum surface adsorbs all the background gas species including H_2, N_2, CO_2.[13] Comparison of these data with the data in Table II makes it possible to visualize (via the partial pressures dynamics) the changes in the sputter surface state that finally affect the $I-V$ curves and the IIEEY behavior. As seen in Table II the H_2 and H peaks with mass numbers 2 and 1 (where H is a water dissociation peak) increase dramatically (101 times) when sputtering occurs. When sputtering is stopped, the peaks smoothly decrease with time. The significant change in hydrogen pressure confirms the idea that the original oxide initially adsorbing the H_2 and H species is removed from the sputter surface during sputtering and the surface becomes pure. The H_2 and H species are no longer adsorbed by either target surface or by deposited aluminum films. This results in the hydrogen accumulation in the gaseous phase. The low hydrogen cryopumping causes the observed increase in the hydrogen partial pressure (Table II). When sputtering is over, an intensive chemisorption occurs. This process then evolves into the time-progressive oxidation with aluminum oxide layer growth. This oxide effectively pumps the hydrogen as well as other background species that causes the final vacuum improvement. Several types of chemical bonds with different bonding energies are known for the chemisorption of H_2O species on aluminum oxide which are susceptible to form sufficiently thick stock of water layers.[15] Although, some residual gas species are not adsorbed at sputtering, the chemisorption of others goes on. As seen in Table II, although the partial pressure of hydrogen jumped more than 100 times during sputtering the pressure of other water species (mass numbers 17, 18) has increased only 17 times. Even taking into account the difference in the molecular cryopumping of the hydrogen and water species this evidence allows us to suppose that some oxygen, including chemisorbed phases, are permanently present on the pure aluminum surface. These phases cause surface structural rearrangement with thin dipole layer formation. In contrast to the high probability of electron scattering in a metal, the scattering in these nonconducting layers is far lower than that which results in an increased electron escape probability.

For polycrystalline targets this adsorbed layer does not uniformly cover the target surface but concentrates in the form of spots around certain crystallographic defects, or on grain boundaries with stronger bonds between adsorbed particles and the surface. In fact, if we compare the $I-V$ characteristics (Fig. 3) we will see that the targets, depending on their grain size, exhibit different $I-V$ curve behavior. The single-crystal target having a sputter surface without grain boundaries, has the highest bias voltage when compared with polycrystalline targets. The grain boundaries decrease the bias voltage, though the effect of grain size on $I-V$ characteristics is not consistent. The target voltage is higher for large and slightly higher for small grain size targets when compared with the medium grain size target. We explain the behavior of the $I-V$ curves by the combined effect of residual gas adsorption and surface grain relief on the resulting IIEEY. This effect is more fully considered in the following section.

IV. IIEEY MEASUREMENT RESULTS AND DISCUSSION

The aluminum single-crystal IIEEY versus ion energy is presented in Table III. As seen, the IIEEY increases only slightly when energy is increased. The small slope of the roughly linear curve confirms the potential type of emission in this particular ion energy range.[16] However, the magnitude of IIEEY are in some contrast with the data presented by Carlston *et al.*,[17] where the IIEEY from the (110) aluminum single crystal at threshold energies (0.9–1 keV) is appreciably higher (0.1) than we measured. This discrepancy may be explained by the effect of surface gas adsorption in Carlston's experiments. A small amount of water vapor introduced into UHV chamber of our apparatus and increased its

TABLE III. Effect of Ar^+ energy and water adsorption on the IIEEY (target temperature 19 °C.)

Ion energy (eV)	IIEEY
600	0.048 ± 0.003
700	0.047 ± 0.003
700 (with oxides)	0.129 ± 0.011
700 (Carlston *et al.* Ref. 17)	0.1
800	0.053 ± 0.005
900	0.057 ± 0.006

Downloaded 23 Dec 2012 to 192.17.144.173. Redistribution subject to AVS license or copyright; see http://avspublications.org/jvsta/about/rights_and_permissions

TABLE IV. Effect of target grain size (GS) and temperature on the IIEEY under 700-eV He^+ bombardment.

Specimen	19 °C	74 °C
Al–1 wt % Cu (GS 0.25 mm)	0.39±0.03	0.48±0.06
Al–1 wt % Cu (GS 0.95 mm)	0.25±0.02	0.36±0.06
Al–1 wt % Cu (GS 5.50 mm)	0.18±0.01	0.23±0.02

partial pressure from 5×10^{-7} to 5×10^{-6} Pa causes the IIEEY to increase to a value nearer the magnitude reported by Carlston *et al.*[17]

The effect of the grain size was studied at temperatures of 19 and 74 °C under the 700-eV He^+ ions bombardment. Light He^+ ions were chosen to increase the IIEEY magnitude. This allow us to increase the measurement accuracy.[16] The temperature of 74 °C was selected to study the IIEEY at actual target sputtering temperatures. The IIEEY as a function of grain size and temperature is presented in Table IV. The temperature effect on the IIEEY is consistent. For all grain sizes (GS), the IIEEY increases when the temperature is raised. An explanation may be found in a close analysis of RGA data taken at the IIEEY measurements. At 74 °C the hydrogen peak is higher than at 19 °C. This suggests that elevated temperatures increase the irreversible reactivity of water dissociation by the formation of water chemisorbed layers. Since the hydrogen does not react with the pure aluminum surface, its partial pressure increases.

The IIEEY continuously increases when the target grain size is changed from large (5 mm) to small (0.25 mm). The small grain size specimen exhibits the greatest IIEEY when compared with the medium and large grain size specimens. However, if we compare the IIEEY data (Table IV) and the $I-V$ characteristics (Fig. 3) a certain difference in trend may be observed. As seen in Fig. 3, the IIEEY from the medium grain size target at sputtering is not appreciably less than the IIEEY from the small grain size target as may be expected from direct IIEEY measurements. In fact the IIEEY from this target is even slightly higher. This difference is explained by the interaction of two competing effects. On one hand an increase in the area of surface grain relief increases the IIEEY due to the residual gas adsorption, on the other hand the surface grain relief decreases the IIEEY due to secondary electron scattering and interception. In the vacuum the adsorption is the only factor affecting the change in the IIEEY, there may be no change in the IIEEY due to change in electron scattering without change in the applied to the sample electrical field. In this case the adsorption effect is largest in the small grain size sample having largest grain boundary area. In the magnetron plasma however it is possible to decrease secondary electron scattering due to plasma penetration into the grain relief cavities.[7] When the sheath thickness matches up with the surface grain relief in size, sheath bending around the relief makes it possible to extend a rather strong electric field into the cavities. This results in the collection of more electrons. This effect is the dominant factor in the case of large grain surface immersed into the plasma. However, the optimal combined effect of these two phenomena which results in increase of the IIEEY and decrease in bias voltage occurs for intermediate grain size reliefs.

V. CONCLUSIONS

The target surface grain size and surface gas coverage affect the sputtering $I-V$ characteristics of polycrystalline aluminum targets. We have shown that the $I-V$ characteristics are sensitive to the IIEEY. For specified sputtering parameters (target crystallographic structure and profile as well as argon pressure and discharge current) the residual gas pressure and grain size associated with target surface temperature are the key parameters affecting the reproducibility of $I-V$ characteristics.

ACKNOWLEDGMENTS

The authors would like to thank C. E. Wickersham, Jr. and J. E. Poole for comprehensive and useful discussion of this work.

[1] L. I. Maissel, in *Handbook of Thin Film Technology*, edited by L. I Maissel and R. Glang (McGraw-Hill, New York, 1970).
[2] D. N. Ruzic, in *Handbook of Plasma Processing Technology*, edited by S. M. Rossnagel, J. J. Cuomo, and W. D. Westwood (Noyes, Park Ridge, NJ, 1990), pp. 70–90.
[3] S. C. Brown, *Basic Data of Plasma Physics* (M.I.T. Press, Cambridge, MA, 1966).
[4] B. Chapman, *Glow Discharge Processes* (Wiley, New York, 1980), pp. 77–133.
[5] S. M. Rossnagel and H. R. Kaufman, J. Vac. Sci. Technol. A **6**, 223 (1986).
[6] S. M. Rossnagel, in Ref. 2, pp. 160–180.
[7] A. Leybovich and T. Kuniya, J. Vac. Sci. Technol. A **11**, 1553 (1993).
[8] J. H. Parker, Jr., Phys. Rev. **93**, 1148 (1957).
[9] H. D. Hagstrum, Phys. Rev. **104**, 1516 (1956).
[10] Y. Takeishi and H. D. Hagstrum, Phys. Rev. **137**, A641 (1965).
[11] C. E. Wickersham, Jr., J. E. Poole, and K. E. Palmer, J. Vac. Sci. Technol. B **4**, 1339 (1986).
[12] P. C. Smith, Ph.D. thesis, University of Illinois, 1993.
[13] P. A. Redhead, J. P. Hobson, and E. V. Kornelson, *The Physical Basis of Ultrahigh Vacuum* (Chapman and Hall, London, 1968).
[14] N. V. Cherepnin, *Sorption Phenomena in Vacuum Technique*, (Sovetskoye Radio, Moscow, 1973) (in Russian).
[15] H. Dunken and P. Fink, Z. Chem. **6**, 194 (1966) (in German).
[16] U. A. Arifov, R. R. Rakhmanov, and K. H. Dzhurakulov, in *Secondary Emission and Structural Properties of Solids*, edited by U. A. Arifov, Translated from Russian by G. D. Archard (New York Consultants Bureau, 1971), pp. 6–10.
[17] C. E. Carlston, G. D. Magnuson, P. Mahadevan, and D. E. Harris, Jr., Phys. Rev. **139**, A729 (1965).

Downloaded 23 Dec 2012 to 192.17.144.173. Redistribution subject to AVS license or copyright; see http://avspublications.org/jvsta/about/rights_and_permissions